epl A Letters Journal Exploring the Frontiers of Physics

June 2021

EPL, **134** (2021) 60001 www.epljournal.org
doi: 10.1209/0295-5075/134/60001

Robust one-way edge state in convection-diffusion systems

L. J. Xu[(a)] and J. P. Huang[(b)]

Department of Physics, State Key Laboratory of Surface Physics, and Key Laboratory of Micro and Nano Photonic Structures (MOE), Fudan University - Shanghai 200438, China

received 13 January 2021; accepted in final form 9 June 2021
published online 17 August 2021

Abstract – Topological insulators are insulated in the bulk but can support edge states on the surface. Since the discovery of edge states in quantum mechanics systems, the related physics has also been extended to classical wave systems. Here, we manage to reveal that edge states are not necessarily limited to wave systems but can also exist in convection-diffusion systems that are essentially different from wave systems. For this purpose, we study heat transfer in a graphene-like (or honeycomb) lattice to demonstrate thermal edge states with robustness against defects and disorders. Convection is compared to electron cyclotron, which breaks space-reversal symmetry and determines the direction of thermal edge propagation. Diffusion leads to interference-like behavior between opposite convection, preventing temperature propagation in the bulk. We also display thermal unidirectional interface states between two lattices with opposite convection. These results extend the physics of edge states beyond wave systems.

Introduction. – Topological insulators were initially discovered in quantum mechanics systems [1,2], which are insulated in the bulk but conductive on the surface. Since the foundation of quantum physics is the Schrödinger wave mechanics, there is a similarity between quantum waves and classical waves in terms of equation forms. Therefore, the concept of topological insulators has also been extended to classical wave systems [3], including but not limited to electromagnetics [4–11] and acoustics [12–21]. The related research was commonly conducted in nonreciprocal systems with the broken time-reversal symmetry induced by an external magnetic bias for electromagnetics [4–6] or an external momentum bias for acoustics [12–16]. Regardless of the quantum or classical description, a feature of topological insulators is that they can support edge states on the surface, which has broad applications for isolators and sensors.

Although edge states have been intensively studied in wave systems, they have received almost no attention in diffusion systems. Unlike wave systems with time-reversal symmetry, diffusion systems feature space-reversal symmetry, indicating that diffusion is identical along two opposite directions. Inspired by topological wave insulators [3] with the broken time-reversal symmetry, it is natural to consider the broken space-reversal symmetry of diffusion systems. Fortunately, several methods are available to break space-reversal symmetry, such as applying asymmetric structures and nonlinear materials [22–25] and considering spatiotemporal modulations [26–29]. Besides symmetry differences, diffusion systems also lack the concept of phase because diffusion generally occurs from high to low potentials, such as from high to low temperatures for heat transfer and from high to low concentrations for mass transfer. To solve the problem, we can introduce a periodic temperature [30–36] for heat transfer or a periodic concentration [37] for mass transfer, which has been experimentally validated [30,31]. With these preliminary analyses, we are able to discuss thermal edge states by considering heat transfer with conduction, as well as convection for breaking space-reversal symmetry. Let us start from the theory.

Theory. – Two basic structures with counterclockwise and clockwise convection are presented in figs. 1(a) and (b), respectively. Convection is an analog of electron cyclotron, which determines the direction of thermal edge propagation, thus called thermal spin herein. For brevity, we regard counterclockwise convection as spin-up and clockwise convection as spin-down. The vertex regions in fig. 1 are solid pumps with high thermal conductivities to drive fluids with convective velocity of v. Besides fluids, convection can also be effectively realized with spatiotemporal modulations of thermal conductivity and density [26–29], which has been experimentally verified to break space-reversal symmetry [28]. Therefore,

(a) E-mail: 13307110076@fudan.edu.cn (corresponding author)
(b) E-mail: jphuang@fudan.edu.cn

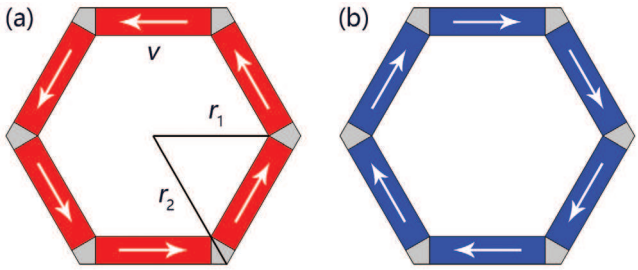

Fig. 1: Two basic structures with inner radius r_1 and outer radius r_2. Vertex regions are solid pumps to drive fluids with (a) counterclockwise velocity and (b) clockwise velocity of v.

what we discuss is a simple and practical system of heat transfer whose governing equation is [38]

$$\rho C\frac{\partial T}{\partial t}+\boldsymbol{\nabla}\cdot(-\kappa\boldsymbol{\nabla}T+\rho C\boldsymbol{v}T)=0, \tag{1}$$

where ρ, C, κ, and $\boldsymbol{v}$ denote density, heat capacity, thermal conductivity, and convective velocity, respectively. T and t represent temperature and time, respectively. $\rho C\boldsymbol{v}$ is the convective term that breaks space-reversal symmetry.

We then need to introduce the concept of phase. For this purpose, we consider a periodic temperature source whose temperature is

$$T=A\mathrm{e}^{-\mathrm{i}\omega t}+B, \tag{2}$$

where A, ω, and B are the temperature amplitude, circular frequency, and reference temperature of the temperature source. The real part of eq. (2) denotes the actual temperature. The temperature source can generate a temperature profile with spatiotemporal periodicity,

$$T=A\mathrm{e}^{\mathrm{i}(\boldsymbol{\alpha}\cdot\boldsymbol{r}-\omega t)}+B, \tag{3}$$

with wave vector $\boldsymbol{\alpha}$ and position vector $\boldsymbol{r}$.

To understand the broken space-reversal symmetry induced by convection, we discuss a one-dimensional case along the x-axis. Since conduction has dissipation, the wave vector should be a complex number, *i.e.*, $\alpha=\beta+\mathrm{i}\gamma$ with wave number β and decay rate γ. The substitution of eq. (3) into eq. (1) yields

$$\beta=\frac{\sqrt{2}\varepsilon}{4}, \tag{4a}$$

$$\gamma=\frac{-8v\omega+2\sqrt{2}v^2\varepsilon+\sqrt{2}D^2\varepsilon^3}{16\omega D}, \tag{4b}$$

with definitions of $\varepsilon=\sqrt{-v^2/D^2+\sqrt{v^4/D^4+16\omega^2/D^2}}$ and $D=\kappa/(\rho C)$. When $v=0$, it is identical along two opposite directions. If $v\neq 0$, a change from v to $-v$ yields the same ε and β but different γ, indicating different decay rates along two opposite directions. Therefore, nonreciprocal temperature propagation can be achieved with convection, which offers an opportunity to realize one-way temperature propagation. Generally speaking, two

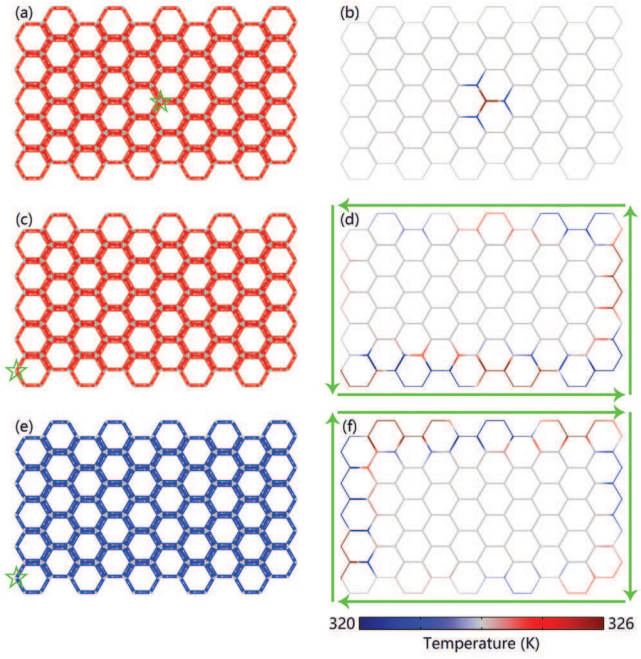

Fig. 2: Thermal edge states. Left and right columns display the structures and simulations at 500 s, respectively. The stars in (a), (c), and (e) denote the positions of periodic temperature sources whose temperatures are $T=40\cos(-\pi t/5)+323\,\mathrm{K}$. The arrows in (d) and (f) show the direction of temperature propagation. The fluids are water with a thermal conductivity of $0.6\,\mathrm{W\ m^{-1}\ K^{-1}}$, a heat capacity of $4200\,\mathrm{J\ kg^{-1}\ K^{-1}}$, and a density of $1000\,\mathrm{kg/m^3}$. The solid pumps are copper with a thermal conductivity of $400\,\mathrm{W\ m^{-1}\ K^{-1}}$, a heat capacity of $390\,\mathrm{J\ kg^{-1}\ K^{-1}}$, and a density of $8900\,\mathrm{kg/m^3}$. $r_1=2-2\sqrt{3}/30\,\mathrm{mm}$ and $r_2=2\,\mathrm{mm}$.

parameters mainly affect temperature propagation: thermal diffusivity determines the decay rate; and convective velocity determines the temperature propagation speed. The chosen parameters are based on water that has a relatively small thermal diffusivity, so dissipation is not that intense and the expected phenomena can still be observed.

Simulation. – We then design a graphene-like (or honeycomb) lattice composed of spin-up units, as presented in fig. 2(a). We firstly discuss the bulk property and put a temperature source in the center (see fig. 2(a)). Each side contains opposite convection in the bulk, so temperature propagation decays far more quickly, as described by eq. (4b). Therefore, the bulk cannot support temperature propagation and becomes insulated (see fig. 2(b)). We then discuss the surface property and put a temperature source at the bottom left corner (see fig. 2(c)). Each side contains only unidirectional convection on the surface, so the decay rate is far lower than that in the bulk. Since the graphene-like lattice is composed of spin-up units, the surface can support only counterclockwise temperature propagation (see fig. 2(d)), which is direct evidence of thermal edge states. Unlike the edge states in wave systems, those in convection-diffusion systems have diffusion-induced

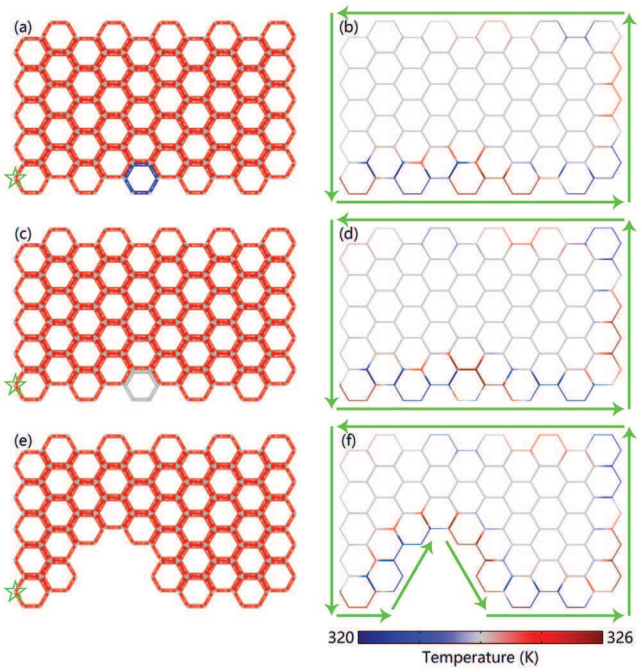

Fig. 3: Robustness against defects and disorders. (a) and (b): reversing a unit. (c) and (d): stopping a unit. (e) and (f): removing six units. The other parameters are the same as those in fig. 2.

dissipation. A simple physical image to understand thermal edge states is that the surface decay rate is far lower than the bulk decay rate, so temperature propagation is allowed only on the surface. To confirm that thermal edge states have directionality, we further construct a graphene-like lattice with spin-down units (see fig. 2(e)). The simulation shows that thermal edge propagation still exists but with clockwise direction (see fig. 2(f)). The results in fig. 2 are in accordance with electron edge states whose propagation directions are determined by electron cyclotrons. Therefore, it is reasonable to compare convection to electron cyclotron despite different mechanisms. In other words, the directions of thermal edge states are locked by thermal spins (*i.e.*, convective directions).

Since edge states are unidirectional, defects and disorders cannot cause backscattering. Analogously, thermal edge states should also be robust against defects and disorders. To confirm this robustness, we perform extended simulations based on the graphene-like lattice. We first change one unit from spin-up to spin-down (see fig. 3(a)). The result indicates that the thermal edge state still exists (see fig. 3(b)), but it has a slightly higher decay rate than fig. 2(d). We then stop one unit from rotating (see fig. 3(c)), and the result is presented in fig. 3(d), demonstrating that the thermal edge state remains unchanged. We finally remove six units from the graphene-like lattice, as displayed in fig. 3(e). Temperature propagation is still allowed only on the surface (see fig. 3(f)). Therefore, the results in fig. 3 prove that thermal edge states

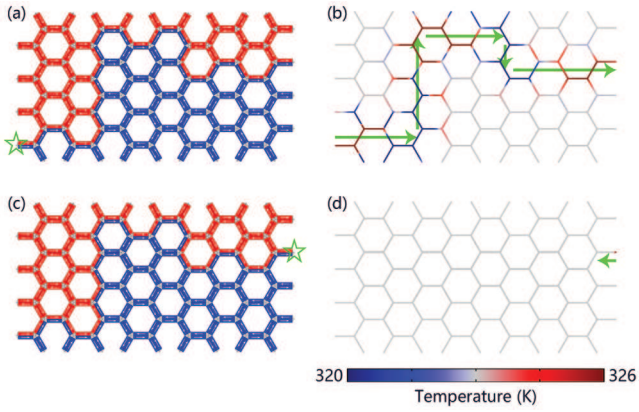

Fig. 4: Thermal interface states. (a) and (b): temperature source at the bottom left corner. (c) and (d): temperature source at the top right corner. The other parameters are the same as those in fig. 2.

are robust against defects and disorders. Moreover, since thermal edge states are robust, the graphene-like lattice is not mandatory and other lattices are also applicable like a square lattice.

We further discuss thermal interface states. In quantum mechanics systems and classical waves systems, the interface between two materials with different topological phases can support topological interface states. Therefore, similar properties should also be applicable to convection-diffusion systems. To reveal thermal interface states, we combine two graphene-like lattices composed of spin-up and spin-down units (see figs. 4(a) and (c)). Since two lattices have different spin directions, unique sides exist at their interface, with the same convective directions. Therefore, the decay rate at the interface is the smallest, which can support temperature propagation (see fig. 4(b)). We also prove the unidirectionality of temperature propagation by putting the temperature source at the output of fig. 4(b), and temperature propagation is forbidden (see fig. 4(d)). Therefore, thermal interface states exist between two lattices with different spin directions. The results in fig. 4 also agree well with the understanding of electron interface states that the interface of two materials with different topological phases is conductive. The simulations in figs. 2–4 prove that the edge states in convection-diffusion systems have properties similar to those in wave systems.

We finally discuss the transition of thermal edge states. For this purpose, we change two parameters of the graphene-like lattice, *i.e.*, the thermal conductivity of the fluid and the circular frequency of the temperature source (see fig. 5(a)). We first change the thermal conductivity of the fluid from $0.6\,\mathrm{W\ m^{-1}\ K^{-1}}$ (water) to $0.001\,\mathrm{W\ m^{-1}\ K^{-1}}$ and $400\,\mathrm{W\ m^{-1}\ K^{-1}}$, and the results are shown in figs. 5(b) and (c), respectively. Both cases become conductive in the bulk and thermal edge states no longer exist. This phenomenon can be explained by the

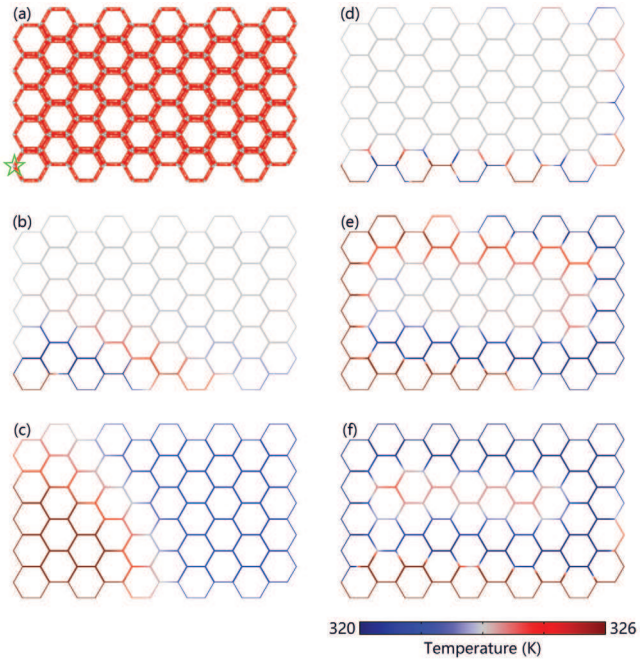

Fig. 5: Transition of thermal edge states. (a) Schematic diagram. Temperature profile with the thermal conductivity of the fluid being (b) 0.001 W m^{-1} K^{-1} and (c) 400 W m^{-1} K^{-1}. Temperature profile with the frequency of the temperature source being (d) $2\pi/5$ rad/s, (e) $\pi/25$ rad/s, and (f) $\pi/50$ rad/s.

decay rate. When the thermal conductivity of the fluid is small (0.001 W m^{-1} K^{-1}), the heat exchange between opposite convection is insufficient, so the decay rate in the bulk is similar to that on the surface, leading to that temperature propagation is allowed both in the bulk and on the surface. When the thermal conductivity of the fluid is large (400 W m^{-1} K^{-1}), the convective term becomes relatively weak and can be ignored. In this way, the broken space-reversal symmetry induced by convection is not obvious, so nonreciprocal propagation almost does not exist. Therefore, the graphene-like lattice not only supports edge states but also supports bulk states. We further discuss the frequency of the temperature source. The periodicity in figs. 5(d)–(f) is 5, 50, and 100 s, respectively. As predicted by eq. (4b), a smaller ω (*i.e.*, a larger periodicity) yields a lower decay rate. Therefore, as ω decreases, the thermal edge state has a larger penetration depth. When the periodicity reaches 100 s, the bulk is almost conductive (see fig. 5(f)). It can also be imagined that when the periodicity tends to infinity ($\omega \to 0$), the graphene-like lattice also supports bulk states, demonstrating the necessity to consider the role of phase (or periodicity).

Discussion and conclusion. – Thermal edge states are closely related to three factors. I) Convection strength, which should be neither too weak nor too strong. If convection is too weak, the broken space-reversal symmetry is not obvious. If convection is too strong, conduction-induced heat exchange between opposite convection is insufficient. II) Temperature frequency. The reason why opposite convection can prevent temperature propagation lies in the interference-like behavior of two temperature waves. If a near-zero temperature frequency is applied (tending to steady states without phase features), the interference-like behavior is not obvious and bulk states can be supported. III) System size. Since temperature amplitude features decay along the propagation direction, a large size causes a large decay. Therefore, we should carefully design these parameters of convection strength, temperature frequency, and system size. Meanwhile, thermal edge states are based on practical materials like water and copper, which can be experimentally realized in principle.

The edge states in convection-diffusion systems are also compared with those in wave systems, and these two types of edge states show similar properties. Therefore, the fundamental origin of thermal edge states might also be topology. However, it is not simple to calculate band structures or Chern numbers in convection-diffusion systems because there is no obvious correspondence between the diffusion equation and the Schrödinger equation. Recent interest in non-Hermitian topology [39–43] may provide some insights. A common approach to a non-Hermitian Hamiltonian is to introduce gain and loss to a Hermitian Hamiltonian. In contrast, diffusion itself features loss, so our system of heat transfer is essentially non-Hermitian [30], which can also be confirmed by the spatial decay of temperature propagation in figs. 2–5. For simplicity, further explorations on non-Hermitian thermal topology might focus on one-dimensional systems at first.

In summary, this work reveals that robust one-way edge states can also exist in convection-diffusion systems. Convection breaks space-reversal symmetry and contributes to one-way temperature propagation. Convection can also be compared to electron cyclotron, which determines the direction of thermal edge propagation. We further confirm the robustness of thermal edge states against defects and disorders. Moreover, we identify thermal interface states between two lattices with different spin directions. Potential applications of thermal edge states can be expected due to the robustness against defects and disorders, such as thermal camouflaging [44–46] and sensing [47–49]. These findings may also guide exploring topological properties with diffusive dynamics and open a new topological diffusion research field, especially topological thermotics.

* * *

We acknowledge financial support from the National Natural Science Foundation of China under Grants No. 11725521 and No. 12035004 and from the Science and Technology Commission of Shanghai Municipality under Grant No. 20JC1414700.

REFERENCES

[1] Hasan M. Z. and Kane C. L., *Rev. Mod. Phys.*, **82** (2010) 3045.
[2] Qi X.-L. and Zhang S.-C., *Rev. Mod. Phys.*, **83** (2011) 1057.
[3] Zangeneh-Nejad F., Alù A. and Fleury R., *C. R. Phys.*, **21** (2020) 467.
[4] Haldane F. D. M. and Raghu S., *Phys. Rev. Lett.*, **100** (2008) 013904.
[5] Wang Z., Chong Y. D., Joannopoulos J. D. and Soljačić M., *Nature*, **461** (2009) 772.
[6] Poo Y., Wu R.-X., Lin Z. F., Yang Y. and Chan C. T., *Phys. Rev. Lett.*, **106** (2011) 093903.
[7] Lu L., Joannopoulos J. D. and Soljačić M., *Nat. Photon.*, **8** (2014) 821.
[8] Christiansen R. E., Wang F. W. and Sigmund O., *Phys. Rev. Lett.*, **122** (2019) 234502.
[9] Ozawa T., Price H. M., Amo A., Goldman N., Hafezi M., Lu L., Rechtsman M. C., Schuster D., Simon J., Zilberberg O. and Carusotto I., *Rev. Mod. Phys.*, **91** (2019) 015006.
[10] Yang Y. H., Gao Z., Xue H. R., Zhang L., He M. J., Yang Z. J., Singh R., Chong Y. D., Zhang B. L. and Chen H. S., *Nature*, **565** (2019) 622.
[11] Hu G. W., Ou Q. D., Si G. Y., Wu Y. J., Wu J., Dai Z. G., Krasnok A., Mazor Y., Zhang Q., Bao Q. L., Qiu C.-W. and Alù A., *Nature*, **582** (2020) 209.
[12] Khanikaev A. B., Fleury R., Mousavi S. H. and Alù A., *Nat. Commun.*, **6** (2015) 8260.
[13] Yang Z. J., Gao F., Shi X. H., Lin X., Gao Z., Chong Y. D. and Zhang B. L., *Phys. Rev. Lett.*, **114** (2015) 114301.
[14] Ni X., He C., Sun X.-C., Liu X.-P., Lu M.-H., Feng L. and Chen Y.-F., *New J. Phys.*, **17** (2015) 053016.
[15] Fleury R., Khanikaev A. B. and Alù A., *Nat. Commun.*, **7** (2016) 11744.
[16] Ding Y. J., Peng Y. G., Zhu Y. F., Fan X. D., Yang J., Liang B., Zhu X. F., Wan X. G. and Chen J. C., *Phys. Rev. Lett.*, **122** (2019) 014302.
[17] Lu J. Y., Qiu C. Y., Ye L. P., Fan X. Y., Ke M. Z., Zhang F. and Liu Z. Y., *Nat. Phys.*, **13** (2017) 369.
[18] Wen X. H., Qiu C. Y., Qi Y. J., Ye L. P., Ke M. Z., Zhang F. and Liu Z. Y., *Nat. Phys.*, **15** (2019) 352.
[19] Souslov A., Dasbiswas K., Fruchart M., Vaikuntanathan S. and Vitelli V., *Phys. Rev. Lett.*, **122** (2019) 128001.
[20] Fan H. Y., Xia B. Z., Tong L., Zheng S. J. and Yu D. J., *Phys. Rev. Lett.*, **122** (2019) 204301.
[21] Qi Y. J., Qiu C. Y., Xiao M., He H. L., Ke M. Z. and Liu Z. Y., *Phys. Rev. Lett.*, **124** (2020) 206601.
[22] Li B. W., Wang L. and Casati G., *Phys. Rev. Lett.*, **93** (2004) 184301.
[23] Li Y., Shen X. Y., Wu Z. H., Huang J. Y., Chen Y. X., Ni Y. S. and Huang J. P., *Phys. Rev. Lett.*, **115** (2015) 195503.
[24] Huang S. Y., Zhang J. W., Wang M., Lan W., Hu R. and Luo X. B., *ES Energy Environ.*, **6** (2019) 51.
[25] Su C., Xu L. J. and Huang J. P., *EPL*, **130** (2020) 34001.
[26] Edwards B. and Engheta N., in *Conference on Lasers and Electro-Optics* (Optical Society of America) 2017, JTu5A.34.
[27] Torrent D., Poncelet O. and Batsale J.-C., *Phys. Rev. Lett.*, **120** (2018) 125501.
[28] Camacho M., Edwards B. and Engheta N., *Nat. Commun.*, **11** (2020) 3733.
[29] Xu L. J., Huang J. P. and Ouyang X. P., *Phys. Rev. E*, **103** (2021) 032128.
[30] Li Y., Peng Y.-G., Han L., Miri M.-A., Li W., Xiao M., Zhu X.-F., Zhao J. L., Alù A., Fan S. H. and Qiu C.-W., *Science*, **364** (2019) 170.
[31] Xu L. J., Wang J., Dai G. L., Yang S., Yang F. B., Wang G. and Huang J. P., *Int. J. Heat Mass Transfer*, **165** (2021) 120659.
[32] Cao P. C., Li Y., Peng Y. G., Qiu C. W. and Zhu X. F., *ES Energy Environ.*, **7** (2020) 48.
[33] Xu L. J. and Huang J. P., *Appl. Phys. Lett.*, **117** (2020) 011905.
[34] Xu L. J. and Huang J. P., *Int. J. Heat Mass Transfer*, **159** (2020) 120133.
[35] Xu L. J. and Huang J. P., *Chin. Phys. Lett.*, **37** (2020) 080502.
[36] Xu L. J. and Huang J. P., *Chin. Phys. Lett.*, **37** (2020) 120501.
[37] Xu L. J., Dai G. L., Wang G. and Huang J. P., *Phys. Rev. E*, **102** (2020) 032140.
[38] Huang J. P., *Theoretical Thermotics: Transformation Thermotics and Extended Theories for Thermal Metamaterials* (Springer, Singapore) 2020.
[39] Parto M., Wittek S., Hodaei H., Harari G., Bandres M. A., Ren J. H., Rechtsman M. C., Segev M., Christodoulides D. N. and Khajavikhan M., *Phys. Rev. Lett.*, **120** (2018) 113901.
[40] Luo X.-W. and Zhang C. W., *Phys. Rev. Lett.*, **123** (2019) 073601.
[41] Kawabata K., Shiozaki K., Ueda M. and Sato M., *Phys. Rev. X*, **9** (2019) 041015.
[42] Okuma N., Kawabata K., Shiozaki K. and Sato M., *Phys. Rev. Lett.*, **124** (2020) 086801.
[43] Borgnia D. S., Kruchkov A. J. and Slager R.-J., *Phys. Rev. Lett.*, **124** (2020) 056802.
[44] Xu L. J., Yang S. and Huang J. P., *EPL*, **131** (2020) 24002.
[45] Li J. X., Li Y., Cao P.-C., Yang T. Z., Zhu X.-F., Wang W. Y. and Qiu C.-W., *Adv. Mater.*, **32** (2020) 2003823.
[46] Xu G. Q., Dong K. C., Li Y., Li H. G., Liu K. P., Li L. Q., Wu J. Q. and Qiu C.-W., *Nat. Commun.*, **11** (2020) 6028.
[47] Han T. C., Yang P., Li Y., Lei D. Y., Li B. W., Hippalgaonkar K. and Qiu C.-W., *Adv. Mater.*, **30** (2018) 1804019.
[48] Xu L. J., Huang J. P., Jiang T., Zhang L. and Huang J. P., *EPL*, **132** (2020) 14002.
[49] Jin P., Xu L. J., Jiang T., Zhang L. and Huang J. P., *Int. J. Heat Mass Transfer*, **163** (2020) 120437.